Radiative recombination in $Cu_2ZnSnSe_4$ thin films with Cu deficiency and Zn excess

M V Yakushev[1,2,3], J Márquez-Prieto[4], I Forbes[4], P R Edwards[1], V D Zhivulko[5], A V Mudryi[5], J Krustok[6] and R W Martin[1]

[1]Department of Physics, SUPA, University of Strathclyde, G4 0NG Glasgow, United Kingdom
[2]Ural Federal University, Mira 19, 620002 Ekaterinburg, Russia
[3]Institute of Solid State Chemistry of Ural Branch of the RAS, Pervomaiskaya 91, 620990 Ekaterinburg, Russia
[4]Northumbria Photovoltaic Application Group, Faculty of Engineering and Environment, Northumbria University, Ellison Place, Newcastle upon Tyne NE1 8ST, United Kingdom
[5]Scientific-Practical Material Research Centre of the National Academy of Science of Belarus, P.Brovki 19, 220072 Minsk, Belarus
[6]Tallinn University of Technology, Departments of Physics and Materials Science, Ehitajate tee 5, 19086 Tallinn, Estonia

E-mail: michael.yakushev@strath.ac.uk

Abstract

Thin films of $Cu_2ZnSnSe_4$ (CZTSe) with copper deficiency and zinc excess were fabricated at Northumbria University by the selenisation of metallic precursors deposited on Mo/glass and bare glass substrates. Absorption and photoluminescence (PL) measurements were used to examine the film on glass whereas films on Mo/glass were used to produce a solar cell with efficiency of 8.1%. Detailed temperature and excitation intensity analysis of PL spectra allows identification of the main recombination mechanisms as band-to-tail and band-to-band transitions. The latter transition was observed in the spectra from 6 to 300 K.

Keywords: $Cu_2ZnSnSe_4$, solar cells, photoluminescence.

1. Introduction

The semiconductor $Cu_2ZnSn(S,Se)_4$ is one of the most promising materials for use as the absorber layer in sustainable thin-film solar cells. It contains cheap and earth abundant elements. Its reported conversion efficiency record exceeds 12% [1] whereas in the pure selenide version $Cu_2ZnSnSe_4$ (CZTSe) it exceeds 11% [2]. The lattice structure as well as the electronic properties of $Cu_2ZnSn(S,Se)_4$ are similar to those in $Cu(In,Ga)Se_2$ (CIGS) [3,4,5]. Such a similarity allows technological solutions, originally developed for CIGS-based solar cells, to be used in CZTSe-based technologies [4].

Intrinsic structural defects, introduced by deviations from the ideal stoichiometry, as with CIGS, are held responsible for the *p*-type doping of CZTSe [4,5]. Although such defects influence charge carrier generation and recombination processes in CZTSe solar cells very little experimental evidence can be found in the literature on the nature of the defects [6-9]. Understanding the electronic properties in this material is mostly based on theoretical studies using density functional theory [5,10] however it is essential to experimentally validate the theoretical findings [4].

Although reported elemental compositions of CZTSe absorber layers, used for solar cells, are rather scattered those in high-performance devices are concentrated at significant deviations from the ideal stoichiometry: copper deficiencies ([Cu]/[Sn+Zn] ratios) as low as 0.8 and zinc excesses ([Zn]/[Sn] ratios) as high as 1.2 [5,11]. At such deviations we can expect the presence of high populations of defects which is hardly compatible with the electrical properties required for high efficiency devices. In CIGSe similar paradox is resolved by efficient mechanisms of electrical passivation of the antisite defect (indium or gallium on copper site, In_{Cu} or Ga_{Cu}), which is the main compensating donor in Cu deficient material. This occurs by formation of the neutral defect complexes $2V_{Cu}+ In_{Cu}$ and $2V_{Cu}+ Ga_{Cu}$, and provides an opportunity to dope CIGS with a shallow acceptor (copper vacancy V_{Cu}) by shifting the elemental composition towards In or Ga excess [12].

Theoretical studies of the possible defect types and their formation energies in CZTSe suggest the presence of similar mechanisms of charge passivation by the formation of donor-acceptor complexes [5]. For copper deficient and zinc excess compositions the defect complexes $V_{Cu}+Zn_{Cu}$ are expected to be formed.

One of the most efficient techniques to study defects in semiconductors is photoluminescence (PL) [13]. The quality and quantity of the information, gained in such studies, critically depends on the structural quality of the studied material [14]. Therefore studies on the highest quality CZTSe provide more information on defects and the electronic properties [6,15]. From the technological point of view it is important to examine PL emission in CZTSe with deviations from stoichiometry required for doping absorbers in efficient solar cells. Low temperature PL spectra of such films reveal a single broad and asymmetrical band attributed to band tail related [7,9,16] and quasi-donor-acceptor pairs [17] recombination. This band usually rapidly quenches with increasing temperature [7] but can be observed up to 180 K in films used as absorber layer in solar cells with high conversion efficiency [9]. On the other hand room temperature PL spectra in such films show an emission band at a spectral energy close to the band gap and assigned to a band-to-band transition [18,19].

However no reports on such a band in CZTSe in low temperature PL spectra or its evolution with temperature can be found in the literature.

In this report we present an optical spectroscopy study of thin films of CZTSe with copper deficiency and zinc excess deposited on glass substrate. Similar CZTSe films, simultaneously deposited on Mo/glass substrates, were used as absorber layers in solar cells with a conversion efficiency of 8.1%. Analysis of the excitation intensity dependence and evolution of the PL spectra with temperature (from 6 to 300 K) and comparison of their spectral energies with the band gap, determined from absorption spectra, helps to identify the recombination mechanism of the dominant emission bands as band-to-tail and band-to-band transitions.

2. Experimental details

Thin films of $Cu_2ZnSnSe_4$ were synthesised at Northumbria University by the selenisation of metallic precursor layers deposited using magnetron sputtering of high-purity elemental targets. These precursors were simultaneously deposited on Mo-coated and bare soda-lime glass substrates at room temperature and then selenised in selenium vapour following a two-step rapid thermal process at 300 ºC and 500 ºC, for 5 and 15 minutes, respectively. Se pellets were used as the chalcogen source. More information on the synthesis of compound films by selenisation of magnetron deposited multilayer metallic precursors can be found in [6,15].

The CZTSe films on Mo/glass substrates were etched with 10 wt% KCN solution for 30 seconds. CdS buffer layers were then deposited on them, using a standard chemical bath process. Solar cells were fabricated by DC-magnetron deposition of ZnO/ZnO:Al transparent front contacts. The principal device parameters for mechanically scribed 3×3 mm^2 solar cells were examined under simulated AM1.5 solar illumination (100 mW/cm^2, 25ºC): V_{oc} = 434 mV, J_{sc} = 31.2 mA/cm^2, FF = 59.6% yielding a conversion efficiency of η = 8.1%.

The films deposited on glass substrates were characterised using a number of techniques.

Their morphology was analysed using a low-vacuum scanning electron microscopy (SEM) and wavelength dispersive X-ray (WDX) microanalysis at 5 and 10 keV electron beam energy, respectively.

The structural properties and the presence of secondary phases were examined by X-Ray diffraction (XRD) measurements carried out using a Siemens D-5000 diffractometer in the Bragg–Brentano geometry and a Cu K-α radiation source (λ = 0.15406 nm).

The temperature and excitation intensity dependent PL measurements were carried out using a 1 m focal length monochromator, the unfocused 514 nm line (0.7 mm diameter) of a 300 mW Ar^+ excitation laser and a closed-cycle helium cryostat. The laser power density on the film was varied from 2.7 mW/cm^2 to 0.13 W/cm^2. The PL signal was detected by an InGaAs photomultiplier tube in the spectral range from 0.9 to 1.7 µm. More experimental details of the set up can be found in [6,15]. Optical transmission and reflection measurements were performed at room temperature in the spectral range from 600 – 1800 nm and used to determine the band gap at room temperature.

3. Results and discussion

The film average thickness of 1.6 µm can be seen in a cross section view of the film shown in figure 1.

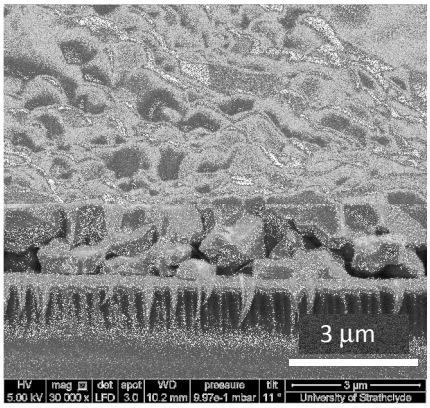

Figure 1. Cross-section view SEM micrograph of the CZTSe film on glass substrate.

The elemental composition (Cu 21.1, Zn 15.1, Sn 13.5 and Se 50.3 at.%) demonstrates a copper deficiency over the Sn and Zn sum [Cu]/[Zn+Sn] = 0.74, excess of zinc over Sn [Zn]/[Sn]=1.12 and nearly stoichiometric ratio of Se to the sum of metals [Se]/[Cu+Zn+Sn] = 1.01.

The XRD pattern, shown in figure 2, reveals distinct lines of a tetragonal CZTSe lattice structure.

Figure 2.XRD pattern of the film on glass substrate.

No significant lines of secondary phases can be seen in the patterns but we cannot rule out the presence of ZnSe and Cu_2SnSe_3because their crystalline structures are quite similar to that of CZTSe [4,16].

Room temperature optical absorption $\alpha(h\nu)$ is calculated using transmittance and reflectance spectra shown in figure 3(a) [20]. For an allowed direct transition the spectral dependence of the absorption coefficient can be calculated as $\alpha=A(h\nu - E_g)^{1/2}/h\nu$, where A is a constant, E_g is the optical band gap and $h\nu$

is the photon energy [21]. Figure 3(b) shows the room temperature dependence of $(\alpha hv)^2$ on hv.

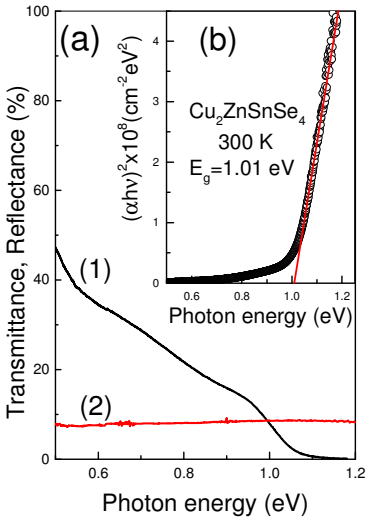

Figure 3. (1) - transmittance and (2) – reflectance measured at room temperature (a), dependence of $(\alpha hv)^2$ on photon energy hv (b).

A band gap of E_g= (1.01±0.02) eV is determined by extrapolating the linear part of $(\alpha hv)^2$ to the hv axis. This value is in a good agreement with E_g = 1.01 eV obtained for high structural quality CZTSe with excitonic features in the PL spectra [6] and suggests a high degree of ordering of Cu and Zn on the lattice [22].

PL spectra measured at different excitation laser power densities at 6 K are shown in figure 4. Features due to water absorption can be seen in the region of 0.9 eV. The spectra are dominated by a broad and asymmetric band BT, labelled for band tail related recombination, with a maximum at 0.94 eV. The high energy side of the BT peak is steeper than the low energy one. The BT band shifts with increasing excitation intensity at a rate (j – shift) of 11 meV per decade of intensity change. Blue shifts of PL bands with increasing excitation power are often used to identify the recombination as being due to donor – acceptor pair (DAP) mechanism. However, the rate of such a j- shift for a DAP cannot exceed a few meV per decade. The significant j-shift, observed for BT, and its asymmetric shape at low temperatures are characteristics of a band-to-tail recombination mechanism [23,24]. The full width at half maximum (FWHM) of the band is about 80 meV. Neither FWHM nor the asymmetric shape changes with excitation intensity. This is due to tails in the electron and hole densities of states, at energies below the conduction band E_c, or above the valence band E_v, which are formed in highly doped semiconductors by spatial potential fluctuations generated by high concentrations of randomly distributed charged defects [25]. A second band at about 1.035 eV, labelled BB, and a low intensity high energy tail HT can also be seen in figure 4. The integrated PL intensity of the sum of the three bands $I(P)$ increases with excitation laser power P as $I \sim P^k$, with a power coefficients of $k \approx 1.2$. Values smaller than unity suggest a recombination involving a process of carrier localisation at defect levels in the band gap whereas values greater than unity suggest excitonic type recombination not involving localisation at defect [26]. Therefore the BT and BB bands can be attributed to transitions not associated with localisation at defect. A value of $k \approx 1.6$ has been reported for the BB and BT bands in the PL spectra of Cu_2ZnSnS_4 [27]. No excitons can be observed in the PL spectra at high doping level of donors because the electron kinetic energy exceeds the Coulomb coupling between electrons and holes [23]. Instead we can expect a band-to-band recombination of free electrons with free holes which can be present as the unresolved BB band in the PL spectra.

An evolution of normalised PL spectra measured at temperatures from 6 to 300 K is shown in Fig. 5 on a linear scale to identify the types of radiative recombination mechanisms. The dominant BT band quenches at temperatures above 100 K, gradually shifting towards lower energies, which indicates that it is associated with the valence band tail [23,24].

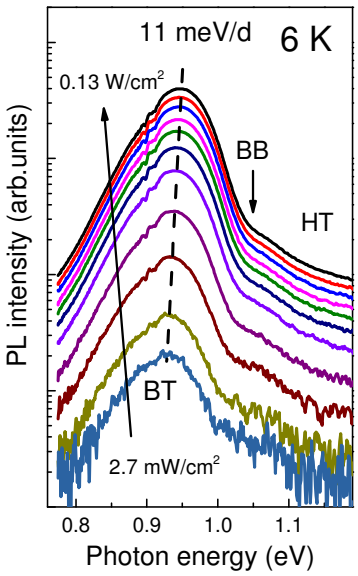

Figure 4. Excitation intensity dependence of PL spectra at 6 K.

The BB band is visible from 6 K. It becomes clearly resolved at 74 K and its intensity remains significant up to room temperature. With temperature increase the BB band shifts towards lower energies as seen in figure 5. The BT and BB bands in the PL spectra have also been reported for Cu_2ZnSnS_4 [27,28].

A semiconductor is highly doped if the average distance between defects is smaller than their Bohr radii, causing the wave-functions of these defects to overlap [25]. Theoretical estimates for CZTSe give the density of state (DOS) hole mass m^*_h= 0.21m_0, where m_0 is the free electron mass, which is significantly heavier than that of the electron m^*_e= 0.08m_0 [10]. Thus the condition of high doping is easier to satisfy for donors whereas heavy holes can be treated as classical particles. In ternary and quaternary chalcopyrite single crystals [24,29] and thin films [30,31], as well as in the

kesterites [7], the condition of high doping is assumed to be satisfied for electrons and not satisfied for holes. At low temperatures holes are localised at deep hydrogenic states of the valence band tail acting like acceptor levels. A PL emission band at 0.94 eV has been reported previously for CZTSe [7,9] and attributed to valence band tail related transitions. An energy diagram with band-to-tail (BT) recombination of free electrons with holes localised at deep valence band tail states, and band-to-band (BB) recombination is shown in figure 6 for a semiconductor with spatial potential fluctuations and the condition of high doping satisfied for donors.

The BT band is broad and has a characteristic asymmetrical shape. The low-energy side of the band is defined by the density of state function of the valence band tail $\rho_v(\varepsilon)$ [23,32]. A good approximation of such a density of states is $\rho_v(\varepsilon) \sim exp(-\varepsilon/\gamma_0)$ [23], where γ_0 is the average depth of the potential energy fluctuations. The low energy side depends neither on temperature nor on excitation intensity, as shown in figure 4 and 5. The high energy side of the band has a more complex nature [23].

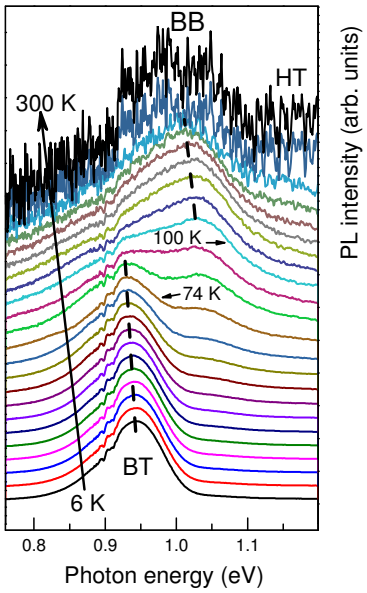

Figure 5. Normalised linear scale dependence of the PL spectra on temperature from 6 to 300 K and shifted for clarity.

It becomes gentler with increase in temperature making the band shape more symmetrical and Gaussian like [24]. The PL spectra at different temperatures were fitted with three Gaussians, corresponding to the BT (near 0.928 eV) and BB (near 1.035 eV) bands as well as a band HT (at 1.121 eV). The fit at 74 K is shown in figure 7. The maxima of the bands and the high energy slopes of the fit are well matched to the spectrum which assists the analysis temperature dependencies of the BB and BT band spectral positions as shown in figure 8. These positions are not affected by mismatch of the fit on the low energy side. The BT peak gradually shifts to lower energies with increasing temperature up to 70 K. The BT band can be assigned to a recombination of free electrons with holes localised at deep valence band tail states as shown in figure 6. At low temperatures free holes are captured at localised tail states. They have a low probability of being released and a higher probability of recombining with free electrons.

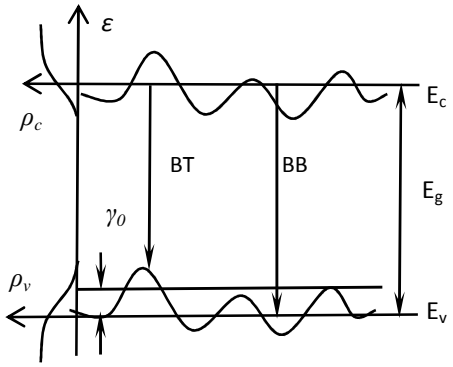

Figure 6. Energy diagram of proposed radiative recombination mechanisms.

Once the temperature increases shallower states begin releasing the holes whereas those at deeper states stay localised causing the observed red shift of the BT recombination [23,24]. At this stage of analysis however we cannot rule out the band-to-impurity (BI) recombination, where free electrons recombine with holes localised at acceptors with ionisation energy greater than γ_0. In materials with spatial potential fluctuations BI also has the characteristic asymmetric shape and red shifts at rising temperature as well as a significant blue shift at increasing excitation intensity [23,29].

Arrhenius analysis of the temperature dependence of the integrated intensity of the BT band after subtraction of the BB and HT bands, is shown in figure 9. The best fit, shown by the line, is achieved for one recombination channel assuming a temperature dependent capture cross section for the localised holes [33]:

$$I(T)=I_0/(1+A_1T^{3/2}+A_2T^{3/2}\exp(-E_a/k_BT)), \quad (1)$$

where I_0 is the band intensity at the lowest temperature, A_1 and A_2 are process rate parameters and k_B is the Boltzmann constant. An activation energy E_a of (13 ± 1) meV is determined. A valence band tail related transition can be described by effective ionisation energy of those acceptor-like states which define the radiative recombination.

In the case of band-to-tail type recombination E_a is a fraction of γ_0. An average tail depth of γ_0 = 37 meV is estimated from the low energy slope of the BT band PL spectrum at 6 K [23,24]. The value of E_a is smaller than γ_0 suggesting that the BT band is more likely to be a band-to-tail type recombination than BI.

The low intensity HT band can probably be related to defects of a secondary phases which can be formed at Zn excess conditions [16,34]. The HT intensity

becomes significant at higher temperatures when the BT band quenches.

The temperature dependence of the BB band, shown in Fig.8, demonstrates a decrease of the spectral energy from 1.035 eV at 74 K to about 1 eV at room temperature. This closely matches the E_g from the absorption experiments so we can consider the BB temperature dependence to follow that of the band gap. The observed 35 meV temperature red shift is close to that of 40 meV observed for excitonic grade CZTSe over a slightly greater temperature change from 4 to 300 K [15] but greater than the 20 meV derived from spectroscopic ellipsometry spectra of a film with lower Cu deficiency and Zn excess [35].

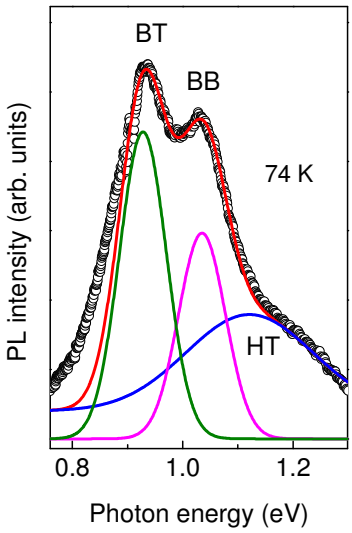

Figure 7. Fitting of the PL spectrum at 74 K with Gaussians representing BT, BB and HT bands.

The high intensity of PL in general and the appearance of the BB transition in a material with copper deficiency and zinc excess at temperatures from 6 to 300 K suggest that despite the presence of band tails, there are low rates of non-radiative recombination and scattering on defects and that the structural quality of the thin film is relatively good.

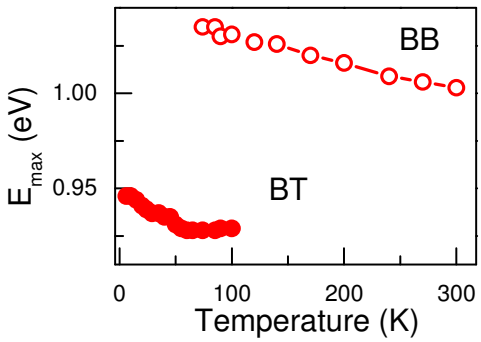

Figure 8. Temperature dependence of the BT and BB band maxima.

Theoretical studies suggest that the defect complexes Zn_{Cu}+Cu_{Zn} and V_{Cu}+Zn_{Cu} influence the CZTSe band gap in an opposite way, the former decreases E_g whereas the latter increases it, which is beneficial for solar cell efficiency [5,36]. Recent nuclear magnetic resonance and Raman spectroscopy report suggests that in copper poor and zinc rich material V_{Cu}+Zn_{Cu} can restrain the Cu/Zn disorder [37]. The proximity of the band gap of 1.00 eV at room temperature to that in excitonic grade material with elemental composition close to ideal stoichiometry [6] showing no band tail effects in the PL spectra can be taken as an indication of a low degree of the Cu/Zn disorder. The presence of the band-to-band transition in the PL spectra from cryogenic to room temperatures and the high conversion efficiency (8.1%) of the solar cell made of the film, simultaneously deposited on Mo/glass substrate with that examined in this study, can also be an indication of the low degree of the Cu/Zn disorder.

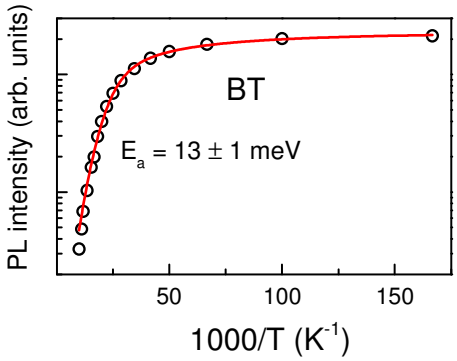

Figure 9.Arrhenius plot of the temperature quenching of the BT band integrated intensity (o- experimental data, red line - fit using Eq.1).

4. Conclusions

CZTSe thin films with copper deficiency and zinc excess have been fabricated by the group at Northumbria University by the selenisation of metallic precursors magnetron deposited on Mo/glass and bare glass substrates. The films on glass were examined by transmission and reflection techniques at room temperature and PL spectroscopy at temperatures from 6 to 300 K whereas films on Mo/glass were used to produce a solar cell with efficiency of 8.1%. Detailed temperature and excitation intensity analysis of the PL spectra allows identification of the main recombination mechanisms as band-to-tail and band-to-band transitions. The latter transition was observed in the spectra from 6 to 300 K.

Acknowledgements

This work was supported by the EPSRC, Royal Society, BRFFR (F15IC-025), the US Civilian Research & Development Foundation (CRDF Global № RUE2-7105EK13) and the Ural Branch of RAS (13CRDF16), RFBR (14-02-00080, 14-03-00121, UB RAS 15-20-3-11), Marie Curie Training Network (ITN), “KESTCELLS”, FP7/2007-2013 grant 316488,

IUT 19-28 of the Estonian Ministry of Education and Research and by FP7 CHEETAH grant 609788.

References

[1] Wang W, Winkler M T, Gunawan O, Gokmen T, Todorov T K, Zhu Y and Mitzi D B 2013 Device characteristics of CZTSSe thin-film solar cells with 12.6% efficiency *Adv. Energy Mater.* **4** 1301465

[2] Lee Y S, Gershon T, Gunawan O, Todorov T K, Gokmen T, Virgus Y and Guha S 2014 $Cu_2ZnSnSe_4$ thin-film solar cells by thermal Co-evaporation with 11.6% efficiency and improved minority carrier diffusion length *Adv. Energy Mater.* **12** 1401372

[3] Romero M J, Du H, Teeter G, Yan Y and Al-Jassim M M 2012 Comparative study of the luminescence and intrinsic point defects in the kesterite Cu_2ZnSnS_4 and chalcopyrite $Cu(In,Ga)Se_2$ thin films used in photovoltaic applications *Phys. Rev.* B **84** 165324

[4] Siebentritt S and Schorr S 2012 Kesterites - a challenging material for solar cells *Prog. Photovolt. Res. Appl.* **20** 512-19

[5] Chen S, Yang J, Walsh A, Gong X G and Wei S H 2013 Classification of lattice defects in the kesterite Cu_2ZnSnS_4 and $Cu_2ZnSnSe_4$ earth-abundant solar cell absorbers *Advanced Materials* **25** 1522 - 39

[6] Luckert F, Hamilton D I, Yakushev M V, Beattie N, Zoppi G, Moynihan M, Forbes I, Karotki A V, Mudryi A V, Grossberg M, Krustok J and Martin R W 2011 Optical properties of high quality $Cu_2ZnSnSe_4$ thin films *Appl. Phys. Lett.* **99** 062104

[7] Grossberg M, Krustok J, Timmo K and Altosaar M 2009 Radiative recombination in $Cu_2ZnSnSe_4$ monograins studied by photoluminescence spectroscopy *Thin Solid Films* **517** 2489-92

[8] Dimitrievska M, Fairbrother A, Saucedo E and Perez-Rodrıguez A 2015 Influence of compositionally induced defects on the vibrational properties of device grade $Cu_2ZnSnSe_4$ absorbers for kesterite based solar cells *Appl. Phys. Lett.* **106** 073903

[9] Queslati S, Brammertz G, Buffiere M, Koble C, Oualid T, Meuris M and Poortmans J 2015 Photoluminescence study and observation of unusual optical transitions in $Cu_2ZnSnSe_4$/CdS/ZnO solar cells *Solar Energy Materials and Solar Cells* **134** 340-5

[10] Person C 2010 Electronic and optical properties of Cu_2ZnSnS_4 and $Cu_2ZnSnSe_4$ *J. Appl. Phys.* **107** 053710

[11] Dmitrievska M, Fairbrother A, Izquierdo-Roca V, Perz-Rodrigues A and Saucedo E 2014 Two ideal compositions for kesterite-based solar cell devices *Proc. 40th IEEE Photovoltaic Conference (PVSC)* 2307-9.

[12] Zhang S B, Wei S -H, Zunger A and Katayama-Yoshida H 1998 Defect physics of the $CuInSe_2$ chalcopyrite semiconductor *Phys. Rev.* B **57** 9642–56

[13] Williams E W and Bebb H B 1972 *Semiconductors and Semimetals*, (R. K. Willardson and A. C. Beer, eds., New York: Academic Press)

[14] Bogardus E H and Bebb H B 1968 Bound-exciton, free-exciton, donor-acceptor and Auger recombination in GaAs *Phys. Rev.* **176** 993-1002

[15] Yakushev M V, Forbes I, Mudryi A V, Grossberg M, Krustok J, Beattie N S, Moynihan M, Rockett A and Martin R W 2015 Optical spectroscopy studies of $Cu_2ZnSnSe_4$ thin films *Thin Solid Films* **582** 154-7

[16] Redinger A, Hönes K, Fontané X, Izquierdo-Roca V, Saucedo E and Valle N 2011 Detection of a ZnSe secondary phase in coevaporated $Cu_2ZnSnSe_4$ thin films *Appl.Phys. Lett.* **98** 101907

[17] Tai K F, GershonT, Gunawan O and Huan C H A 2015 Examination of electronic structure differences between CIGSSe and CZTSSe by photoluminescence study *J. Appl. Phys.* **117** 235701

[18] Redinger A, Sendler J, Djemour R, Weiss T P, Rey G, Dale P J and Siebentritt S 2015 Different band gaps in $Cu_2ZnSnSe_4$: A high temperature Co-evaporation study *IEEE Journal of Photovoltaics* **5** 641-8

[19] Collord A D, Xin H and Hillhouse H W 2015 Combinatorial exploration of the effects of intrinsic and extrinsic defects in $Cu_2ZnSn(S,Se)_4$ *IEEE Journal of Photovoltaics* **5** 288-98

[20] Mudryi A V, Gremenok V F, Victorov I A, Zalesski V B, Kurdesov F V, Kovalevski V I, Yakushev M V and Martin R W 2003 Optical characterisation of $CuInSe_2$ thin films synthesised by two-stage selenisation process *Thin Solid Films* **431/432** 193-6

[21] Pankove J I 1975 *Optical Processes in Semiconductors* (Dover Publications, Inc. New York)

[22] Krämmer C, Huber C, Zimmermann C, Lang M, Schnabel T, Abzieher T, Ahlswede E, Kalt H and Hetterich M 2014 Reversible order-disorder related band gap changes in $Cu_2ZnSn(S,Se)_4$ via post- annealing of solar cells measured by electroreflectance *Appl. Phys. Lett.* **105** 262104

[23] Levanyuk A P and Osipov V V 1981 Edge luminescence of direct-gap semiconductors *Soviet Physics Uspekhi* **24** 187-215

[24] Krustok J, Collan H, Yakushev M and Hjelt K 1999 The role of spatial potential fluctuations in the shape of the PL bands of multinary semiconductor compounds *Physica Scripta* T **79** 179-82

[25] Shklovskii B I and Efros A L 1984 *Electronic Properties of Doped Semiconductors* (Berlin: Springer)

[26] Schmidt T, Lischka K and Zulehner W 1992 Excitation-power dependence of the near-band-

edge photoluminescence of semiconductors *Phys. Rev.* B **45** 8989-94

[27] Grossberg M, Salu P, Raudoja J and Krustok J 2013 Micro-photoluminescence study of Cu_2ZnSnS_4 polycrystals *J. Photon. Energy* **3** 030599

[28] Tanaka M, Shinji T, Uchiki H 2014 Photoluminescence from Cu_2ZnSnS_4 thin films with different compositions fabricated by a sputtering-sulfurization method *Solar Energy Materials and Solar Cells* **126** 143-8

[29] Jagomagi A, Krustok J, Raudoja J, Grossberg M, Danilson M and Yakushev M 2003 Photoluminescence studies of heavily doped $CuInTe_2$ crystals *Physica* B **337** 369–74

[30] Dirnstorfer I, Wagner M, Hofmann D M, Lampert M D, Karg F and Meyer B K 1998 Characterization of $CuIn(Ga)Se_2$ thin films *Physica status solidi (a)* **168** 163-75

[31] Yakushev M V, Mudryi A V, Gremenok V F, Zaretskaya E P, Zalesski V B, Feofanov Y and Martin R W 2004 Influence of growth conditions on the structural quality of $Cu(InGa)Se_2$ and $CuInSe_2$ thin films *Thin Solid Films* **451** 133-6

[32] Bhattacharya R, Pal B and Bansal B 2012 On conversion of luminescence into absorption and the van Roosbroeck-Shockley relation *Appl. Phys. Lett.* **100** 222103

[33] Krustok J, Collan H and Hjelt K 1997 Does the low-temperature Arrhenius plot of the photoluminescence intensity in CdTe point towards an erroneous activation energy? *J. Appl. Phys.* **81** 1442-5

[34] Luckert F, Yakushev M V, Martin R W, Beattie N, Zoppi G, Moynihan M, Forbes I, Mudryi A V, Karotki A V and Krustok J 2010 Optical properties of thin films of $Cu_2ZnSnSe_4$ fabricated by sequential deposition and selenisation Proceeding of the 6th Photovoltaic Science, Applications and Technology, University of Southampton, The Solar Energy Society UK 29-32

[35] Choi S G, Kim T J, Hwang S Y, Li J, Persson C, Kim YD, Wei S-H and Repins I L 2014 Temperature dependent band-gap energy for $Cu_2ZnSnSe_4$: A spectroscopic ellipsometric study *Solar Energy Materials and Solar Cells* **130** 375-9

[36] Huang D and Persson C 2013 Band gap change induced by defect complexes in Cu_2ZnSnS_4 *Thin Solid Films* **535** 265-9

[37] Washio T, Nozaki H, Fukano T, Motohiro T, Jimbo K and Katagiri H 2011 Analysis of lattice site occupancy in kesterite structure of Cu_2ZnSnS_4 films using synchrotron radiation x-ray diffraction *J. Appl. Phys.* **110** 074511